THE ATLAS ELECTRON AND PHOTON TRIGGER PERFORMANCE IN LHC RUN 2

D. Maximov, on behalf of the ATLAS Collaboration

[1] *Budker Institute of Nuclear Physics, 11 Akademika Lavrentieva st., Novosibirsk, 630090, Russia*

[2] *Novosibirsk State University, 1 Pirogova st., Novosibirsk, 630090, Russia*

E-mail: Dmitriy.Maximov@cern.ch

ATLAS electron and photon triggers covering transverse energies from 5 GeV to several TeV are essential to record signals for a wide variety of physics: from Standard Model processes to searches for new phenomena in both proton-proton and heavy ion collisions. The main triggers used during LHC Run 2 (2015–2018) for those physics studies were a single-electron trigger with E_T threshold around 25 GeV and a diphoton trigger with thresholds at 25 and 35 GeV. Relying on those simple, general-purpose triggers is seen as a more robust trigger strategy, at a cost of slightly higher trigger output rates, than to use a large number of analysis-specific triggers. To cope with ever-increasing luminosity and more challenging pile-up conditions at the LHC, the trigger selections needed to be optimized to control the rates and keep efficiencies high. The ATLAS electron and photon trigger performance during Run 2 data-taking is presented as well as work ongoing to prepare for the even higher luminosity of Run 3 (2021–2023).

Keywords: ATLAS, HLT, EGamma

Dmitriy Maximov

1. Introduction

Electrons and photons are present in many Standard Model processes as well as in searches for phenomena beyond the Standard Model. This paper presents the evolution of the performance of the ATLAS electron and photon triggers in LHC Run 2 (2015 to 2018).

2. The ATLAS detector and its trigger system

ATLAS [1] is a multipurpose detector designed to observe particles produced in high-energy proton–proton (pp) and heavy-ion (HI) collisions. It is composed of a tracking detector (ID) in the innermost region around the interaction point, surrounded by calorimeters and muon chambers.

A two-level trigger system [2] is used to select events of interest. The first-level (L1) trigger utilises signals from the calorimeters and the muon chambers to reduce the event rate from the 40 MHz bunch crossing rate to below 100 kHz. L1 also defines regions-of-interest (RoIs) which have calorimeter clusters with high transverse energy, E_{T}, or muon tracks in the muon chambers.

Events accepted by L1 are processed by the high-level trigger (HLT), based on algorithms implemented in software which must further reduce the number of events recorded to disk to an average rate of about 1 kHz. The HLT uses fine-granularity calorimeter information, precision measurements from the muon spectrometer and tracking information from the ID, which are not available at L1.

3. Electron and photon trigger reconstruction

Electron and photon reconstruction at the HLT stage is performed on each ElectroMagnetic Calorimeter (EM) RoI provided by the L1. It proceeds in a series of sequential steps composed by a set of algorithms, so that if it fails at a certain step, subsequent steps are not executed. In the HLT, fast algorithms are executed first, allowing precision algorithms to run at a reduced rate later in the trigger sequence.

Fast algorithms are executed using calorimeter and ID information within the RoI to perform the initial selection and identification of the electron and photon candidates, and achieve early background rejection.

If a particle candidate satisfies the criteria defined for the fast selection, the precision algorithms are executed in the HLT. These precision online algorithms are similar to their offline counterparts [5], with the following exceptions: the bremsstrahlung-aware re-fit of electron tracks (GSF) [3] and electron and photon dynamic, variable-size topo-clusters [4, 5] are not used online; photon candidates are identified using only the calorimeter information online; online and offline use different metrics to account for pile-up (the number of interactions per bunch crossing) and some other minor differences [6].

Since 2017 the neural-network-based Ringer algorithm [6] was introduced into the Fast step of the electron triggers with E_{T} threshold > 15 GeV, it exploits the property of EM showers to develop in the lateral direction in an approximately conical structure around the initial particle, see Figure 1 (left).

The Ringer algorithm increases the time taken by the fast calorimeter reconstruction step, however, it reduces the number of input candidates for the more CPU-demanding fast tracking step. Overall, the use of the Ringer algorithm enabled at least a 50% reduction in the CPU demand, while keeping the total trigger efficiency the same, as shown in Figure 1 (right).

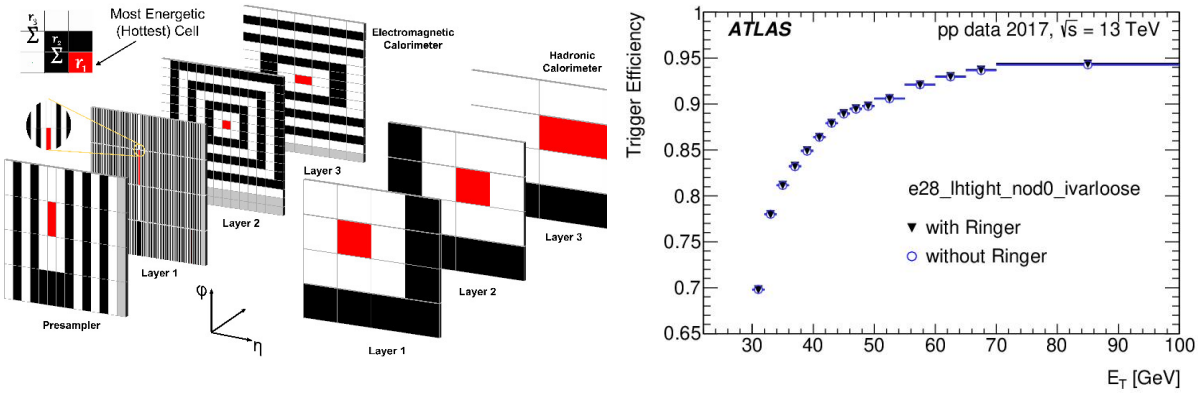

Figure 1. The Ringer algorithm concept (left) and performance (right) [6]

4. Performance of electron and photon triggers during Run 2

Table 1, with notation defined in [6], shows the lowest-threshold unprescaled photon triggers in different data-taking periods during Run 2. An optimisation of the selection for the online 'tight' definition was performed at the end of 2017 in order to synchronise with a reoptimised offline 'tight' photon selection.

Table 1. List of unprescaled triggers with photons in different pp data-taking periods during Run 2. The corresponding L1 trigger threshold is given in brackets. From [6]

Trigger type	**2015**	**2016**	**2017–2018**
Single photon	g120_loose (EM22VHI)	g140_loose (EM22VHI)	
Primary diphoton	g35_loose_g25_loose (2EM15VH)		g35_medium_g25_medium (2EM20VH)
Loose diphoton			2g50_loose (2EM20VH)
Tight diphoton	2g20_tight (2EM15VH)	2g22_tight (2EM15VH)	2g20_tight_icalovloose (2EM15VHI)

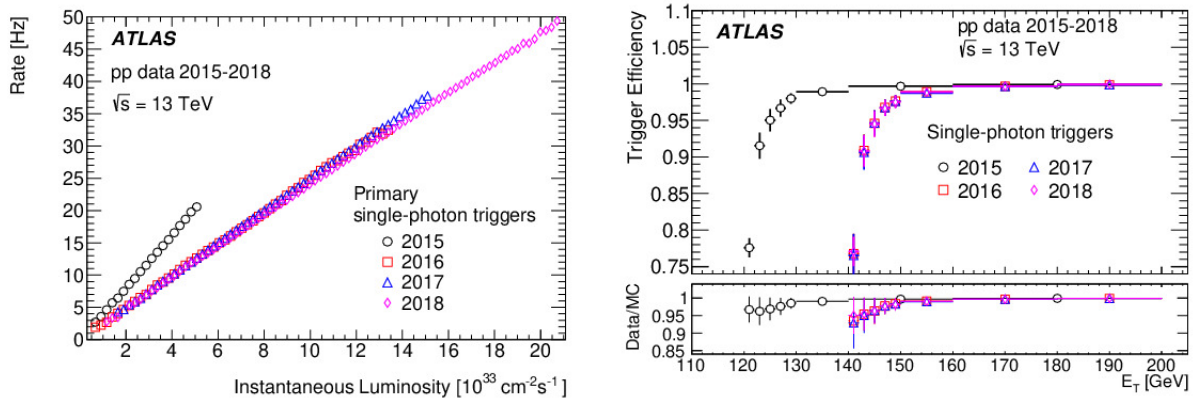

Figure 2. Photon trigger evolution and performance [6]

The trigger rates and efficiencies of the single-photon triggers in 2015–2018, measured with the Bootstrap method [6], are shown in Figure 2 as a function of instantaneous luminosity and E_T. The total uncertainties, shown as vertical bars, are dominated by systematic uncertainties, especially

differences between data and Monte Carlo simulation. The trigger efficiency measurement has a total uncertainty of the order of 1% for photons with E_T values 5 GeV above the trigger threshold, and an uncertainty of less than 0.1% for photons at least 10 GeV above the trigger threshold.

The evolution of the Run 2 electron trigger thresholds for the main unprescaled triggers is summarised in Table 2, with notation defined in [6].

Table 2. List of unprescaled electron triggers in different pp data-taking periods during Run 2. The corresponding L1 trigger threshold is given in brackets. From [6]

Trigger type	**2015**	**2016**	**2017–2018**
Single electron	e24_lhmedium (EM20VH) e120_lhloose e200_etcut	e26_lhtight_nod0_ivarloose (EM22VHI) e60_lhmedium_nod0 e140_lhloose_nod0 e300_etcut	
Dielectron	2e12_lhloose (2EM10VH)	2e17_lhvloose_nod0 (2EM15VH)	2e17_lhvloose_nod0 (2EM15VHI) 2e24_lhvloose_nod0 (2EM20VH)

Figure 3 shows the rates for the lowest-threshold unprescaled isolated single-electron triggers used during Run 2 as a function of the instantaneous luminosity. The offline electron is required to pass the 'tight' identification and 'FCTight' isolation requirements [5]. The sharper efficiency turn-on as a function of E_T in 2015 shown in Figure 3 is due to a looser identification requirement and no isolation requirement. Although similar identification, isolation, and E_T requirements are imposed in the single-electron triggers in 2016–2018, some inefficiency at E_T < 60 GeV is observed in 2016. This is explained by the different electron trigger configuration used in 2016, in particular the inefficiency of the calorimeter-only likelihood (LH) selection at the precision step [6]. The trigger efficiency at E_T < 60 GeV was recovered from 2017 by the introduction of a data-driven LH selection and a looser fast selection with the Ringer algorithm.

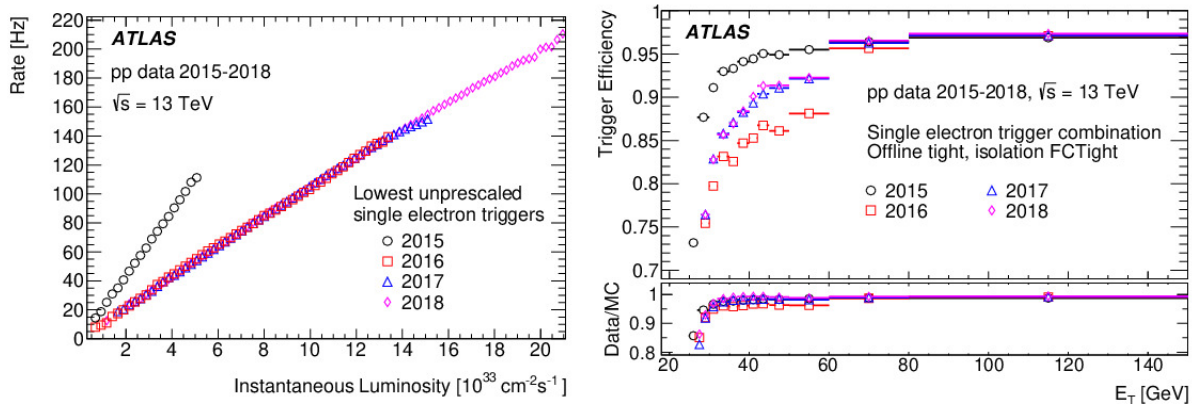

Figure 3. Performance evolution of single electron trigger [6]

The primary unprescaled photon trigger used in 2015 and 2018 lead-lead (PbPb) data-taking had a 20 GeV E_T threshold, and the photon candidate was required to satisfy 'loose' identification criteria. Figure 4 shows the 2018 photon trigger efficiency using the Bootstrap method. The efficiency is shown as a function of Forward Calorimeter (FCal) $\sum E_T$, with and without underlying event (UE) subtraction applied in the online reconstruction. When the reconstruction does not include UE subtraction, i.e. in the same manner as done in pp collision data-taking, the efficiency shows a strong dependence on collision centrality. When the reconstruction uses the UE subtraction procedure, the photon trigger efficiency remains high across the full range of centralities. The (offline, calibrated) photon-E_T dependence of photon trigger efficiencies using UE subtraction are shown for photon triggers with 15 and 20 GeV E_T thresholds. The efficiency is determined with respect to offline reconstructed photons which pass a tighter set of identification cuts, identical to those used in typical

physics analyses. The HI photon triggers become fully efficient at about 5 GeV above the nominal online trigger threshold, similar to the photon triggers used for the pp data-taking.

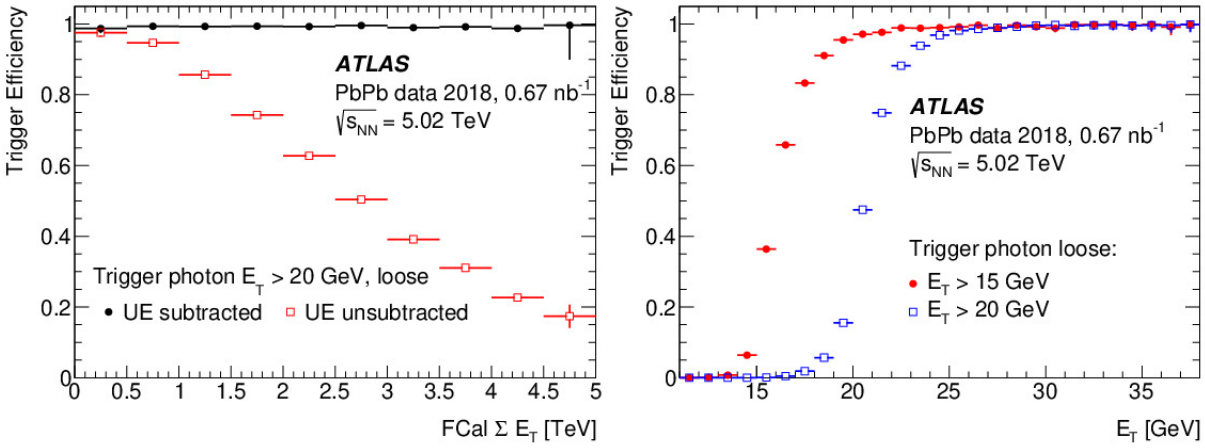

Figure 4. Photon trigger efficiencies as a function of FCal $\sum E_T$ and offline photon E_T. The error bars indicate statistical uncertainties only [6]

4. Conclusions

The ATLAS electron and photon triggers and their evolution during LHC Run 2 are described. To cope with a fourfold increase of peak LHC luminosity in Run 2 (2015–2018), to 2.1×10^{34} cm^{-2} s^{-1}, trigger algorithms and selections needed to be optimised to control the trigger rates and CPU usage while retaining a high efficiency for offline analyses.

For future data-taking, using more features from offline reconstruction algorithms (Gaussian Sum Filter [3], Superclusters [5]) are expected to improve energy and momentum resolution at the trigger stage.

References

[1] ATLAS Collaboration, The ATLAS Experiment at the CERN Large Hadron Collider, JINST 3 (2008) S08003.

[2] ATLAS Collaboration, Performance of the ATLAS trigger system in 2015, Eur. Phys. J. C 77 (2017) 317, arXiv: 1611.09661 [hep-ex].

[3] ATLAS Collaboration, Improved electron reconstruction in ATLAS using the Gaussian Sum Filter-based model for bremsstrahlung, ATLAS-CONF-2012-047, 2012, url: https://cds.cern.ch/record/1449796.

[4] ATLAS Collaboration, Topological cell clustering in the ATLAS calorimeters and its performance in LHC Run 1, Eur. Phys. J. C 77 (2017) 490, arXiv: 1603.02934 [hep-ex].

[5] ATLAS Collaboration, Electron and photon performance measurements with the ATLAS detector using the 2015–2017 LHC proton–proton collision data, (2019), arXiv: 1908.0005 [hep-ex].

[6] ATLAS Collaboration, Performance of electron and photon triggers in ATLAS during LHC Run 2, (2019), arXiv: 1909.00761 [hep-ex]